Rock Mech. Rock Engng. (2002) 35 (1), 45–64

Rock Mechanics and Rock Engineering

Strength and Deformational Behaviour of a Jointed Rock Mass

By

M. Singh[1], **K. S. Rao**[2], and **T. Ramamurthy**[2]

[1] Civil Engineering Department, IIT, Roorkee, India
[2] Civil Engineering Department, IIT, New Delhi, India

Summary

An assessment of the strength and deformational response of jointed rock masses is an essential requirement in the site selection, design and successful execution of Civil and Mining Engineering projects. A quick estimate of these properties for preliminary evaluation of alternate sites, will reduce considerable expenditures for field tests. An attempt has been made in the present study to develop a link between strength and deformability of jointed block masses with the properties of intact specimens, obtained from simple laboratory tests, taking into account the influence of the properties of the joints. Extensive experimentation has been carried out on large specimens of jointed block masses under uniaxial compression. The model material represents a low strength rock. Various joint configurations were introduced to achieve the most common modes of failure occurring in nature. A coefficient called Joint Factor has been used to account for the weakness brought into the intact rock by jointing. Methods of computing the Joint Factor for various modes of failure of a jointed mass in an unconfined state have been established. The effect of Joint Factor on strength and tangent modulus of the mass has been studied and the values have been correlated with those of intact rock. Guidelines for assessing probable modes of failure of a jointed mass will enable one to estimate the relevant strength and tangent modulus of the mass.

Symbols

θ: Inclination of joint with horizontal,
β: Inclination of joint w.r.t direction of loading,
$\sigma_{ci,\,cj}$: Uniaxial compressive strength of intact and jointed rock mass,
σ_{cr}: σ_{cj}/σ_{ci},
ϕ_j: Friction angle along the critical joints,
a, b: Empirical coefficients for predicting strength and tangent modulus of jointed mass,
$E_{i,j}$: Tangent modulus of intact and jointed rock mass,
E_r: E_j/E_i,
J_f: Joint Factor,
J_n: Number of joints/m depth in direction of loading,
n: Joint inclination parameter,
r: Joint strength parameter.

1. Introduction

A fair assessment of strength and deformational behaviour of jointed rock masses is necessary for the design of slopes, foundations, underground openings and anchoring systems. Both the intact rock and the properties of the joints govern the mass response. If the mass is not highly fractured and the joint system has only few sets (say five or less), then the mass usually behaves anisotropically. Surface or near surface activities in rock mass occur under low confining pressure. In such cases the influence of joints is quite predominant. The uncertainty in predicting the behaviour of a jointed mass under uniaxial stress is essentially caused by scale effects and the unpredictable nature of the modes of failure. Extensive field tests are often required to assess the strength and deformability of the ground making the exercise quite expensive. To minimise this uncertainty an extensive experimental study has been carefully planned and executed to develop a more reliable link between the strength and modulus of jointed rock masses and those of the intact rock.

2. Experimental Programme

The experiments were conducted on specimens of a jointed block mass (Singh, 1997) formed of saw cut blocks of a model material. The joint configuration was varied to achieve the possible modes of failure commonly occurring in the field. The details of the experimental programme are as follows:

2.1 Model Material

For reproducibility of results and ease of working, a model material called Sand-lime brick was used in this study. The material has a uniaxial compressive strength (UCS) of 17.13 MPa and represents a weak rock belonging to the "EM" group on the Deere-Miller (1966) classification chart. The physical and engineering properties of the material are presented in Table 1.

Table 1. Properties of the model material

Property	Value
Dry density, γ_d(kN/m^3)	16.86
Porosity (%)	36.94
UCS, σ_{ci} (MPa)	17.13
Brazilian strength, σ_{ti} (MPa)	2.49
Tangent modulus, E_i (GPa)	5.34
Poisson's ratio, ν_i	0.19
Cohesion, c_i (MPa)	4.67
Friction angle of intact material, ϕ_i°	33.00
Friction angle along the Joints, ϕ_j°	37.00
Deere-Miller classification (1966)	EM

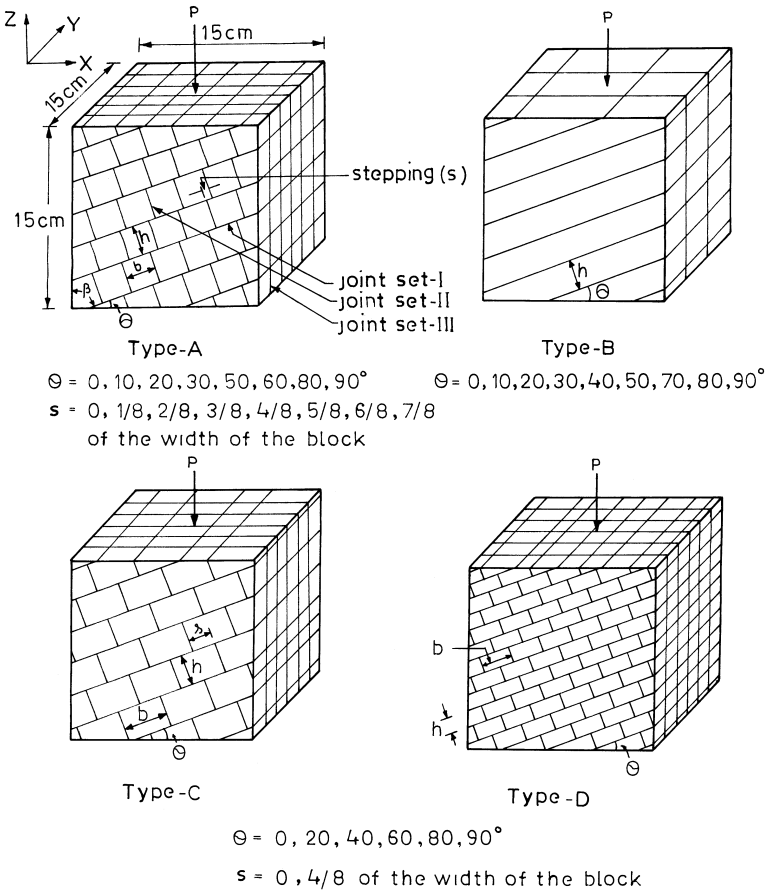

Fig. 1. Configuration of joints tested

2.2 Description of Specimens of Jointed Block Mass

The jointed specimens can be grouped into two main categories (see Fig. 1). The first category belongs to Type-A specimens in which the specimens were formed from cubical blocks. The major part of the experimental programme belongs to Type-A specimens. A few additional tests were conducted by varying the geometry of the elemental blocks forming the specimens (Types-B, C and D).

2.2.1 Type-A Specimens

A typical configuration of the specimens is shown in Fig. 1. To have a reasonably scale free jointed block mass, it was decided to have at least six elements in each direction. The size of each of the specimens was $15 \times 15 \times 15$ cm and on an average there were more than 260 cubes, each of 2.5 cm side length. The jointed mass

consisted of three sets of joints. The joints in Set-I were continuous and inclined at a variable angle θ, with the horizontal. The values of θ adopted were 0, 10, 20, 30, 50, 60, 80 and 90°. The joints in Set-II were orthogonal to Set-I and were staggered at variable stepping 's'. For each orientation θ, the values of 's' used were 0, 1/8, 2/8, 3/8, 4/8, 5/8, 6/8 and 7/8 of the width of the block. The joint Set-III remained vertical. A total of 55 specimens were tested in this category.

2.2.2 Types-B, C and D Specimens

Few selected tests were also conducted with changed geometry of the elemental blocks forming the specimens. Three more geometries were investigated (Fig. 1). In Type-B, plates of 2.5 cm thickness (h) were used. The values of θ adopted for Type-B specimens were 0, 10, 20, 30, 40, 50, 70, 80 and 90°. A total of nine specimens were tested in this category.

The Type-C specimens had block width, $b = 3.75$ cm and height, $h = 2.5$ cm ($h/b = 0.67$). The Type-D specimens had blocks with dimensions as $b = 2.5$ cm and $h = 1.25$ cm ($h/b = 0.5$). For both Types-C and D, the orientation θ was adopted as 0, 20, 40, 60, 80 and 90°. For each orientation only two steppings i.e. zero and 4/8 (half of the width of the block) were used. For Types-C and D, 12 specimens of each were tested.

2.3 Preparation of the Specimens and Testing Programme

The bricks of the model material were cut into plates and bars and then into blocks or cubes as per the requirement of the specimen. These blocks or cubes were then arranged on a perspex sheet with required orientation and stepping 's' (Fig. 2a). All four sides were cut to obtain one vertical segment of the jointed specimen (separated by joint Set-III). All the six segments were prepared using the same method and oven dried at 105 °C for 24 hours. After this, the blocks were kept in air for 7 days and on the eighth day they were assembled to form the specimen for testing. To minimise end friction two sandwiches of Teflon sheets smeared with silicon grease were used at the top and the bottom of the specimen. Eight rubber bands of low stiffness were placed around the specimen to hold the blocks in place. Four LVDTs were used to measure the vertical deformation between the upper and lower loading platens (Fig. 2b). Horizontal deformations were measured at the centre of all the four vertical faces of the specimen using LVDTs. The tests were conducted under uniaxial stress conditions. Load was applied through a hydraulic jack under controlled rate of deformation. The rate of loading was so adjusted that the failure took place within 20 minutes from starting of the experiment. The deformations were continued till the load decreased to about half to one third of the peak load. The mode initiating the failure was recorded and failure patterns were photographed. From sorting of bricks to the completion of testing the jointed specimen, a time span of about 20 days was required.

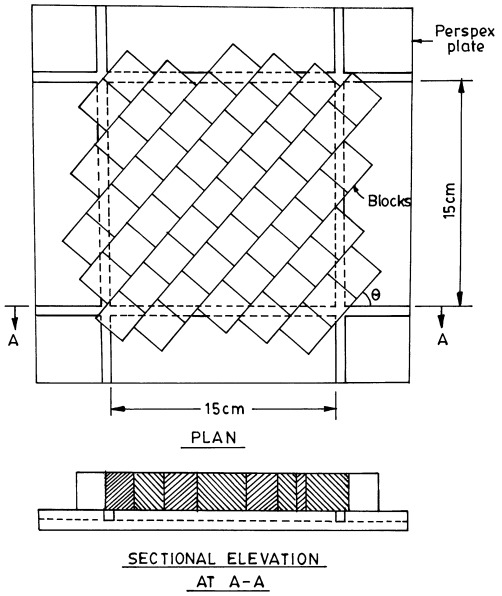

Fig. 2a. Plan and front view (sectional) of the blocks arranged to be cut for desired joint configuration

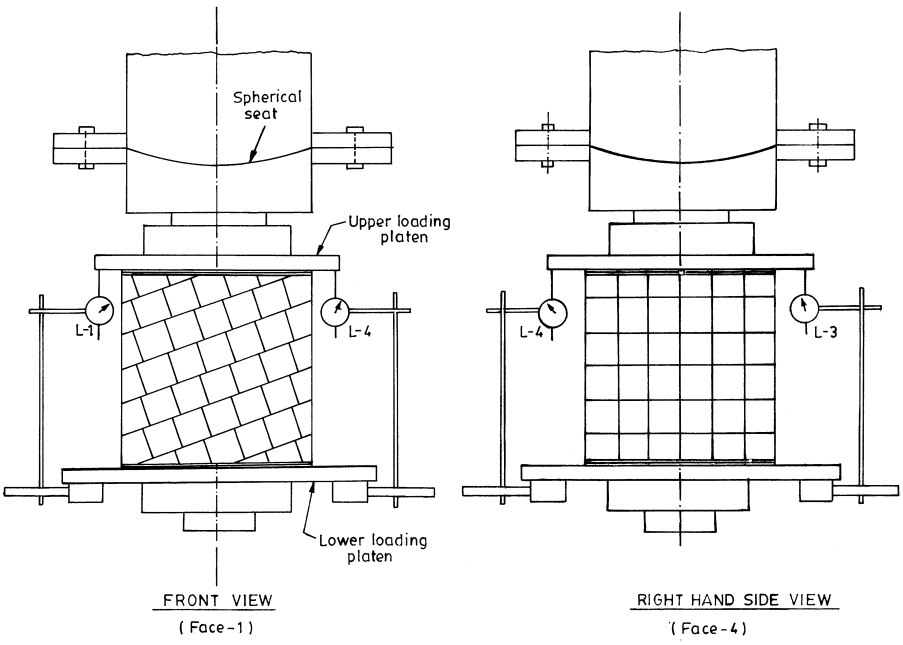

Fig. 2b. Schematic diagram of arrangement of LVDTs to measure the vertical deformation

3. Results and Discussion

3.1 Modes of Failure

The modes of failure of the jointed block specimens have been complex and combinations of more than one mechanism occur. It was however possible to identify the most dominant mode initiating the failure. Out of all the combinations available, four distinct modes of failure were identified viz.: *Splitting* of intact material, *shearing* of intact material, *rotation* of blocks and *sliding* along critical joints (Fig. 3).

3.1.1 Splitting

The term splitting implies failure of material due to tensile stresses developed within it. The failed specimens show large number of minute cracks, roughly vertical in direction and without any sign of shearing. The crushing of material is also considered under this mode.

3.1.2 Shearing

The specimen fails due to one or more shearing planes, which are inclined and pass through the intact material and the pre-existing joints. Signs of displacement along

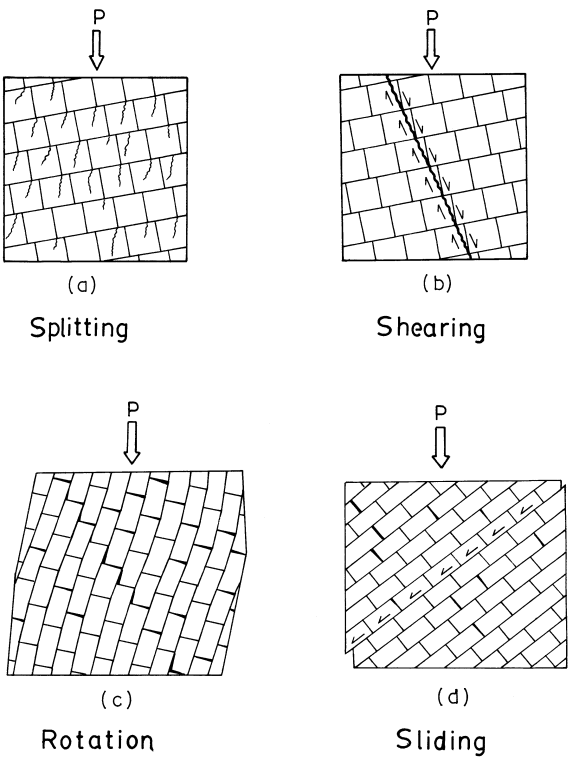

Fig. 3. Sketches of the modes of failure

Table 2. Zones of modes of failure for Type-A specimens

90	***Shearing***							
80	***Rotation***							
70	***Sliding***							
50								
40								
30								
20				***Shearing***				
10								
0	***Splitting***							
θ° ↑ s→	0	1/8	2/8	3/8	4/8	5/8	6/8	7/8
	Nil	Low		Medium		High		V. high
	Extent of Interlocking →							

the shearing plane are shown by the specimen. Gouge material is also formed due to shearing.

3.1.3 Rotation

Under this mode of failure rotation of blocks takes place right from the beginning of the experiment. The specimen as a whole translates and large relative displacement in the transverse direction is observed. The elemental material remains intact.

3.1.4 Sliding

The specimen failure was initiated due to sliding on the continuous joints. The mode is associated with large deformations, stick-slip phenomena and a poorly defined peak in the stress-strain curves. At large deformations the mode is mostly associated with either rotation or material failure or any other complex combination of modes.

A summary of the modes of failure observed for Type-A specimens is presented in Table 2. The table shows distinctly different regions in terms of orientation of joints and stepping conditions (a measure of interlocking), in which a particular mode of failure lies. This was also confirmed by modes of failure obtained for other types of specimens. The observations from this table are used later to suggest guidelines for assessing the mode of failure in the field.

3.2 Stress-Deformation Response

The axial stress has been computed by applying corrections for changes in the cross sectional area due to lateral expansion during loading. Axial strains were corrected for the compression of the Teflon sandwiches. The compressive stress and strains are considered positive. Most of the stress-strain curves are S-shaped and some of them are presented in Fig. 4. Out of the two deformations measured in the transverse directions, the deformation in the direction X (Fig. 1) is generally larger due to dipping of joints. Near the origin, the axial stress-strain curve is

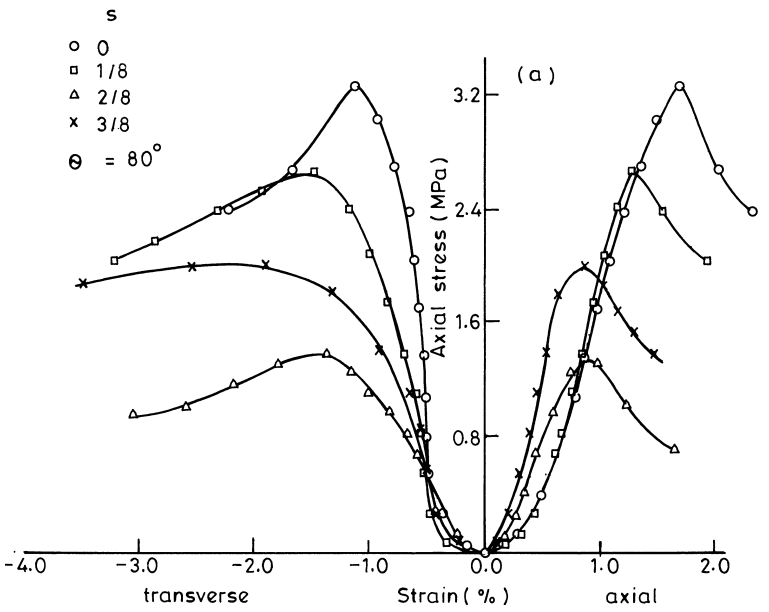

Fig. 4. Few typical stress-strain curves (Type-A specimens)

concave upward, which indicates closure of joints and an initial seating effect. The middle portion of all the curves is linear, exhibiting elastic deformations. The failure of the specimens was progressive, and near the peak did not show a sudden stress decrease. For almost all cases of splitting, shearing and rotational mode of failure, smooth stress-strain curves were obtained. In the sliding mode, the specimens failed exhibiting stick-slip phenomena along the joints.

3.3 Effect of Interlocking on Strength and Deformational Behaviour

The strength and deformational characteristics are found to change with different combinations of inclination of joints, θ, and interlocking, 's'. The effect of stepping 's' on strength and tangent modulus for Type-A specimens is shown in Fig. 5 (a and b). These values are shown in terms of ratios as defined below:

$$\sigma_{cr} = \sigma_{cj}/\sigma_{ci}, \tag{1}$$

$$E_r = E_j/E_i. \tag{2}$$

Where, σ_c and E refer to the uniaxial compressive strength and tangent modulus respectively; the subscripts i and j refer to intact and jointed specimens respectively. From the observations of the test results, the following conclusions are drawn:

i. Stepping has little effect on the strength when the continuous joints are horizontal or vertical ($\theta = 0°$ and $90°$). The specimens fail either due to splitting or shearing through intact material, giving upper bound values of strength and tangent modulus. There is no systematic influence of stepping and the properties are thus primarily influenced by joint frequency.

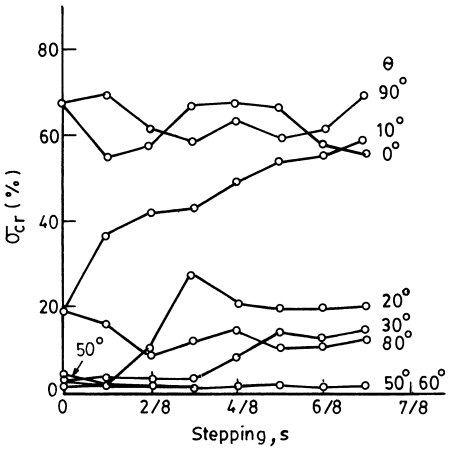

Fig. 5a. Effect of stepping '*s*' on the strength of the jointed block mass (Type-A specimens)

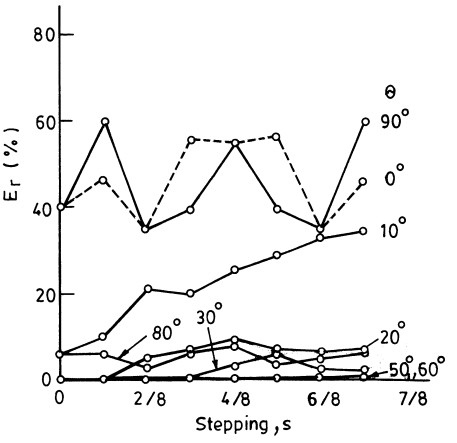

Fig. 5b. Effect of stepping '*s*' on the tangent modulus of the jointed block mass (Type-A specimens)

ii. For the range of $0° < \theta \leq 30°$, the drastic changes in mode of failure are found to occur. For the same inclinations of joints the mode of failure varied from one extreme i.e. sliding along the critical joints to the other i.e. splitting or shearing of intact material depending on the interlocking produced by stepping. The mode of failure influenced the engineering properties sharply for the same orientation of joints due to increased interlocking. The values of σ_{cj} and E_j in general increase with stepping and attain the maximum values, where the mode of failure shifts to shearing or splitting i.e. at '*s*' near to 2/8, 3/8 and 5/8 for $\theta = 10°$, 20° and 30° respectively. Beyond these steppings the increase in σ_{cj}, E_j is nominal.

iii. The increase in σ_{cj} and E_j due to stepping is maximum for $\theta = 10°$ but as θ approaches a value of 30°, this increase becomes smaller and smaller.

iv. For $\theta \approx 10°$, and $s = 6/8$ and 7/8 the increase in strength due to stepping is so high that the values become similar to those for $\theta = 0°$ and 90°. The effect of inclination of joints can thus be ignored if the joints are slightly inclined with the horizontal and the mass is highly interlocked. The interlocking however, does not improve the tangent modulus to the same extent. For structures where high deformability is acceptable, provided the mass has sufficient strength (as in the case of mining situations) this aspect may be quite important.

v. For the specimens with θ in the range of 50° and 60°, the value of σ_{cj} and E_j are the lowest; and the failure strains are maximum due to sliding. There is no effect of stepping on these values. These are the orientations where the effect of inclination of joints is more dominant than the interlocking of the joints.

vi. If the mass has a single set of joints and it is oriented critically ($\theta \approx 50°$ to 60°), the mass will have almost negligible strength and sliding may occur due to weight of the mass itself.

vii. For $\theta = 80°$, rotation is the characteristic mode of failure. The values of σ_{cj} and E_j are higher than for sliding but still very low.

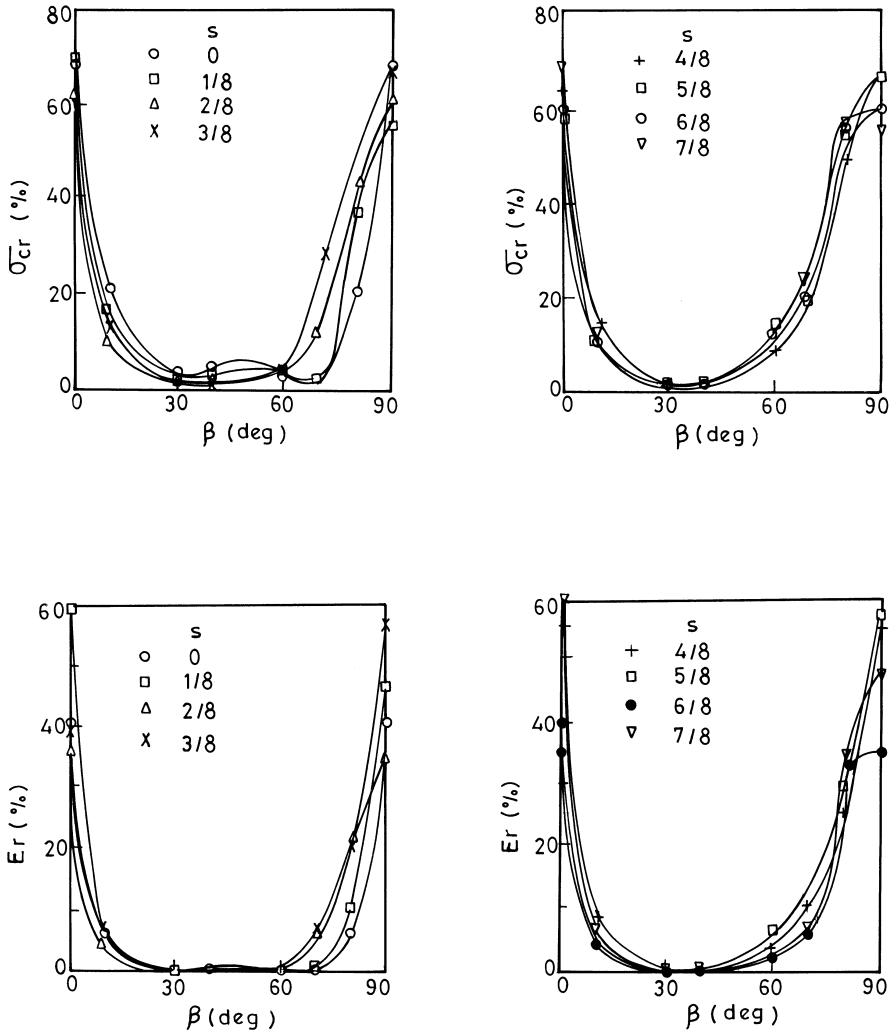

Fig. 6. Anisotropic behaviour in strength and tangent modulus (Type-A specimens)

3.4 Anisotropic Behaviour

One of the most important features of the joints in rock is that they introduce anisotropy in strength and deformability. If there is a large number of joint sets (say five or more) the mass may again behave somewhat isotropically provided that no set has a dominant effect. The anisotropy introduced by joints on strength and deformability of jointed specimens is discussed next.

3.4.1 Type-A Specimens

The variation of strength and tangent modulus for Type-A specimens with inclination is shown in Fig. 6. The properties have been plotted against the angle

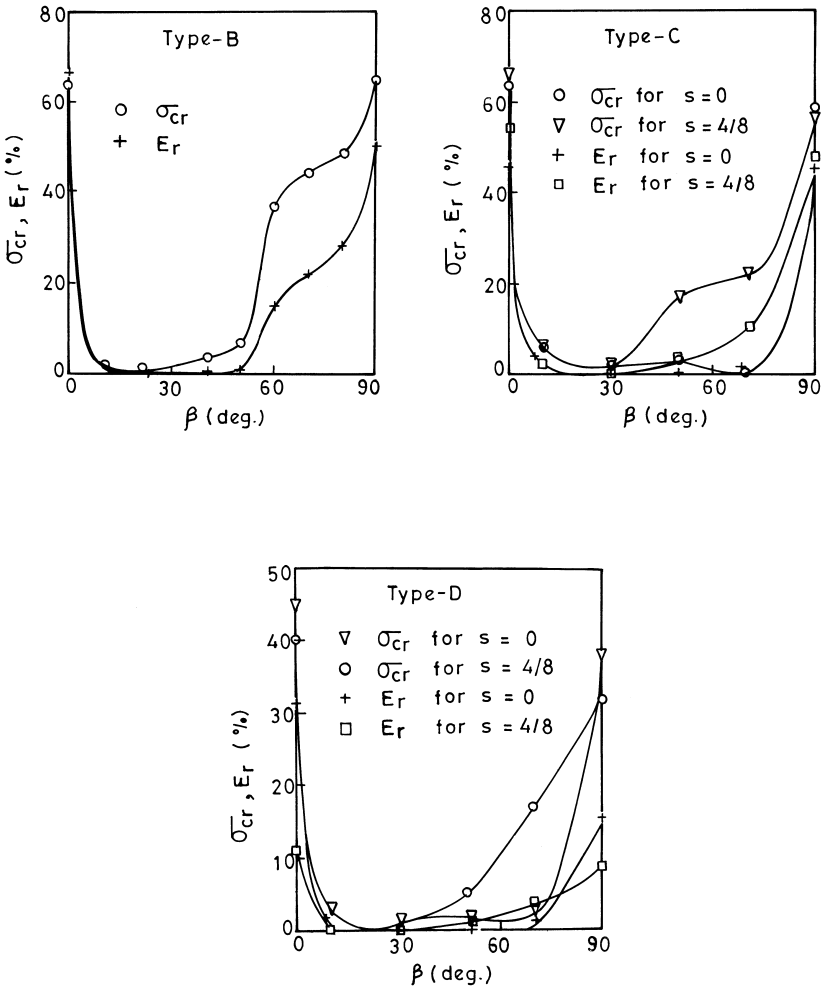

Fig. 7. Anisotropic behaviour in strength and tangent modulus (Type-B, C and D specimens)

β, which is the orientation of continuous joints relative to the loading direction, $(90 - \theta^\circ)$. It is observed that the values of σ_{cr} $(= \sigma_{cj}/\sigma_{ci})$ and E_r $(= E_j/E_i)$ drop sharply between $\beta = 0^\circ$ to 30° with minimum at 30°. There is no effect of stepping on the shape of the curve in this range of β values. For $\beta > 30^\circ$, the properties start increasing and attain maximum values at $\beta = 90^\circ$. In the range of $\beta = 30^\circ$ to 90° an effect of stepping on the shape of the curve is observed. For $s = 0$, the values continue to be minimum till $\beta = 60^\circ$ and then increase to reach maximum at $\beta = 90^\circ$. The shape of the curve resembles the letter 'U' with a flat base.

3.5 Types-B, C and D Specimens

The Type-B specimens had single set of joints and showed a maximum drop of values between $\beta = 0$ to 10° (Fig. 7). The steeply inclined single set of joints may

be thus more unstable. It is so because, the blocks rotate about their bases as columns hinged at their respective bases. Anisotropic curves for Type-B specimens are of U-shape, with very low values between $\beta = 10$ to 50°.

The Type-C specimens ($h/b = 0.67$) were tested with two steppings only i.e. $s = 0$ and $4/8$. For $s = 0$ the variation for σ_{cr} and E_r is represented by flat based U-shaped curve having high values at $\beta = 0^\circ$ and 90° only (Fig. 7). For all other orientations, these values were small. For strength, substantial increase is observed for $\beta > 30^\circ$ due to higher interlocking.

The Type-D ($h/b = 0.5$) specimens were also tested with two steppings only. For strength, observations similar to Type-C were made. The difference is that the strength values are in general low as compared to Type-C specimens. This is due to higher frequency of joints used for this type. The variation of σ_{cr} with β is U-shaped with a very wide base for $s = 0$, and shifts towards V-shape due to interlocking for $s = 4/8$ (Fig. 7). The E_r values were also quite low due to high frequency of joints. The effect of frequency of joints on E_r is so prominent, that no appreciable increase in the value is observed at $s = 4/8$ for $\beta > 30^\circ$.

4. Concept of Joint Factor

The influence of jointing on the response of intact rock can be studied through a weakness coefficient called Joint Factor (Ramamurthy, 1993; Ramamurthy and Arora, 1994). This coefficient reveals the ''weakness'' brought in to the intact rock through jointing and takes into account the combined effect of frequency of joints, their inclination and roughness along the critical joints. The higher the Joint Factor, the greater is the ''weakness''. It is defined taking the three key factors controlling the response of the jointed mass into account.

$$J_f = \frac{J_n}{n.r}, \tag{3}$$

where J_f = Joint Factor;

J_n = number of joints/m depth in the direction of loading;

n = critical joint inclination parameter presented in Table 3. The parameter was derived by conducting experiments on specimens with inclined joints (Ramamurthy, 1993; Ramamurthy and Arora, 1994).

r = sliding joint strength parameter = $\tan\phi_j$; where ϕ_j is friction angle along the critical joint at sufficiently low normal stress so that the initial roughness of the surface is reflected through this value.

Table 3. The value of inclination parameter, n (Ramamurthy, 1993)

Orientation of joint β°	Inclination parameter n	Orientation of joint β°	Inclination parameter n
0	0.810	50	0.306
10	0.460	60	0.465
20	0.105	70	0.634
30	0.046	80	0.814
40	0.071	90	1.000

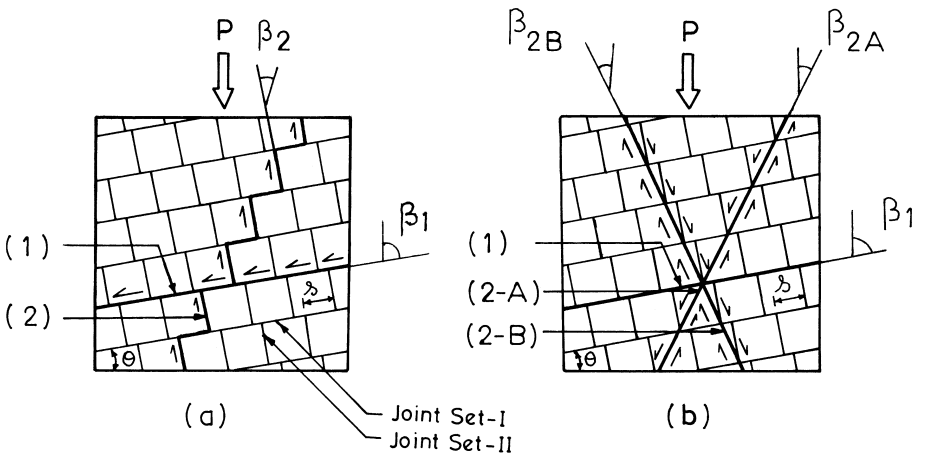

Fig. 8. Potential failure surfaces to compute J_f

For the present study, the value of ϕ_j was computed by conducting direct shear tests on the joint surface between the two bocks. The experimental data were subdivided based on the failure mode, and the following methods were used to compute the parameters J_n and n and hence J_f.

4.1 Splitting Mode of Failure

i. A section of the rock mass is drawn to scale (Fig. 8a).
ii. All the potential failure surfaces belonging to type (1) are marked. Only one such surface is shown in the figure. The number of these surfaces per metre depth in vertical direction (J_n) is computed.
iii. The inclination β_1 is read, and the corresponding value of inclination parameter is assigned from Table 3.
iv. J_f for potential failure surface (1) is computed by using the above values.
v. Another section of the mass is drawn, and all the potential failure surfaces of type (2) (Fig. 8a) are marked. Their number per metre depth (J_n) is computed. The inclination parameter is assigned corresponding to angle β_2 (Fig. 8a) and J_f is computed for potential failure surface (2).
vi. The higher value of J_f obtained above is considered critical and used for analysis.

4.2 Shearing Mode of Failure

i. The section of the rock mass is drawn to scale (Fig. 8b).
ii. All the potential failure surfaces belonging to type (1) are marked. J_f for surface (1) is computed as per the procedure explained for splitting mode of failure.

iii. Another section is drawn and two potential failure surfaces of the types (2-A) and (2-B) through the bases of the angularities formed by stepping, are marked as shown in the figure. The angles β_{2A} and β_{2B} are computed/measured and only the surface having an angle β near the value $45^\circ - \phi_j/2$ is selected for computing J_f.
iv. All the potential failure surfaces belonging to the type selected above (either 2-A or 2-B) are marked. Their frequency in the vertical direction is computed to give J_n and the inclination parameter is assigned as per their inclination. J_f is thus computed for potential failure surfaces designated as (2-A) or (2-B).
v. Out of the values of J_f computed above, the maximum is considered critical.

4.3 Rotational Mode of Failure

i. The section of the rock mass is drawn to scale. All the potential failure surfaces belonging to type (1) are marked as shown in Fig. 8b. J_f for surface (1) is computed as discussed above.
ii. If joint Set-II is stepped, a method similar to that for the shearing mode of failure is adopted and J_f is computed for the potential failure surface either (2-A) or (2-B).
iii. If stepping is zero, then only surface (2-A) is considered along the joint Set-II and J_f is computed.
iv. The maximum value of J_f is considered critical.

4.4 Sliding Mode of Failure

i. The section of the rock mass is drawn to scale.
ii. Only the surface (1) is considered and J_f is computed as discussed in previous cases (Fig. 8a).

5. Effect of Joint Factor on Strength and Tangent Modulus

The computed J_f values as derived above are used to investigate their influence on the strength and tangent modulus of the jointed mass. The ratios (σ_{cr} and E_r) are plotted against J_f. The following observations are made for different modes of failure:

5.1 Splitting Mode of Failure

The variations of σ_{cr} and E_r with J_f for the specimens tested in the present investigation are shown in Figs. 9 (a and b). It is observed that J_f has a decisive effect on the values of σ_{cr} and E_r, which decrease exponentially with increasing J_f. The following correlations are found to exist.

$$\sigma_{cr} = \sigma_{cj}/\sigma_{ci} = \exp(-0.0123 J_f), \tag{4}$$

$$E_r = E_j/E_i = \exp(-0.020 J_f). \tag{5}$$

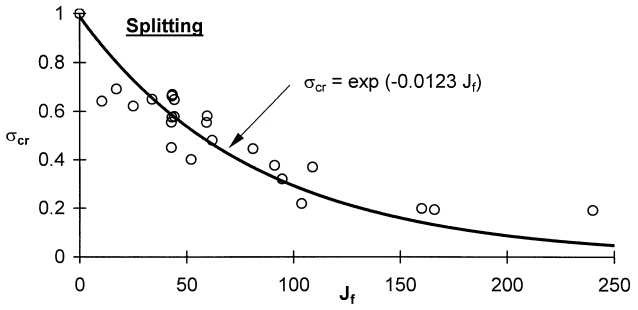

Fig. 9a. Variation of σ_{cr} with J_f for splitting mode of failure

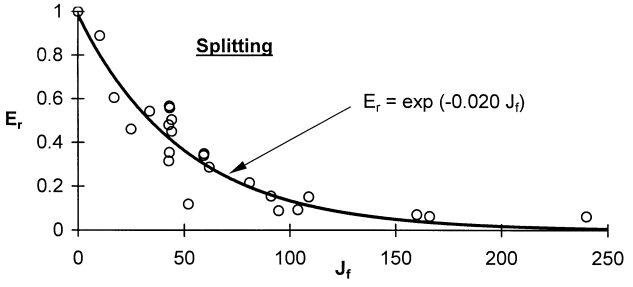

Fig. 9b. Variation of E_r with J_f for splitting mode of failure

5.2 Shearing Mode of Failure

The effect of J_f on experimental values of σ_{cr} and E_r is shown through Fig. 10 (a and b). It is found that σ_{cr} and E_r decrease with increasing J_f upto about $J_f \approx 200$; beyond this the variations are negligibly small. The variation can be represented as:

$$\sigma_{cr} = \exp(-0.011 J_f), \tag{6}$$

$$E_r = \exp(-0.020 J_f). \tag{7}$$

5.3 Rotational Mode of Failure

This mode of failure is highly influenced by the geometry of the blocks forming the specimens. The variation of strength and modulus for Type-A specimens (square shaped geometry) are shown in Fig. 11 (a and b). The σ_{cr} values though small in magnitude, show a decreasing trend with increasing J_f. The first experimental point for jointed specimens is at $J_f \approx 60$. There are no experimental points available below this value of J_f. Using the theoretical point at $J_f = 0$ (representing intact rock), the best fitting curves are shown in the figures. The correlations for Type-A specimens are obtained as:

$$\sigma_{cr} = \exp(-0.025 J_f), \tag{8}$$

$$E_r = \exp(-0.04 J_f). \tag{9}$$

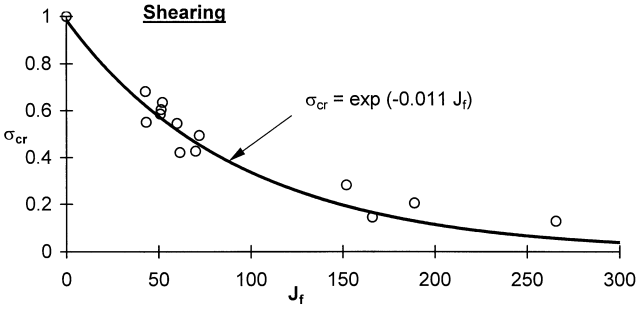

Fig. 10a. Variation of σ_{cr} with J_f for shearing mode of failure

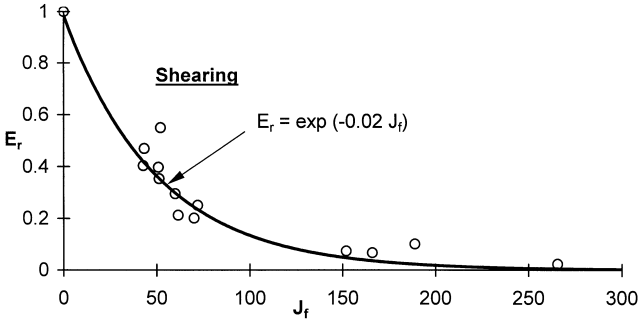

Fig. 10b. Variation of E_r with J_f for shearing mode of failure

For the specimens with block geometries other than square shaped, it is not possible to show any correlation due to inadequate number of data points available.

5.4 Sliding Mode of Failure

The effect of J_f on the strength and modulus for specimens failing due to sliding along critical joints are shown in Figs. 12 (a and b). Very low values of σ_{cr} and E_r are obtained for this mode. The following correlations are obtained for the specimens tested in the present study:

$$\sigma_{cr} = \exp(-0.018 J_f), \tag{10}$$

$$E_r = \exp(-0.035 J_f). \tag{11}$$

6. Prediction of the Engineering Response of a Jointed Rock Mass

To predict the strength and deformation of jointed rock masses in an unconfined state, the geometric data about the joints will have to be collected by joint map-

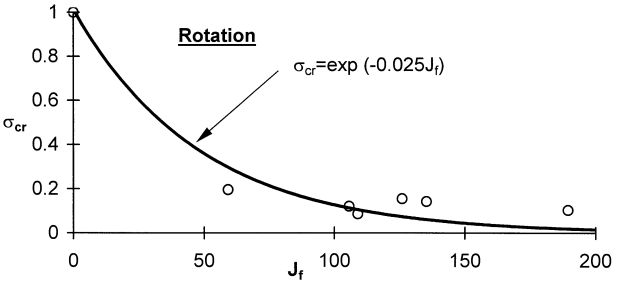

Fig. 11a. Variation of σ_{cr} with J_f for rotational mode of failure

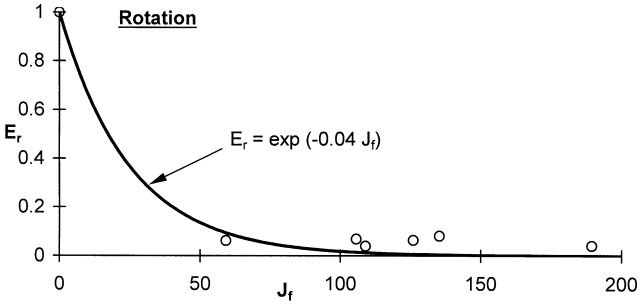

Fig. 11b. Variation of E_r with J_f for rotational mode of failure

ping. These surveys will yield the frequency, inclination and condition of joints. Direct shear tests along joints will be required to compute the joint shearing resistance. In the absence of shear tests, approximate values can be assigned as suggested by Ramamurthy (1993). The response of the mass will depend on the mode of failure likely to occur in the field. The probable mode of failure in the field can be assessed based on the guidelines suggested below.

6.1 Guidelines for Probable Mode of Failure

A rough estimate of the probable mode of failure in the field is made based on the test results presented in Table 2. It is assumed that the mass has two sets of joints, out of which one is continuous and the other is either at a low, intermediate, or high level of interlocking as per the assessment of the investigator. Also the mass is considered to be under uniaxial stress conditions and the problem is treated in two dimensions only. The guidelines to assess the probable mode of failure are as follows:

i. If the continuous joints are horizontal, the mass is expected to fail due to splitting.

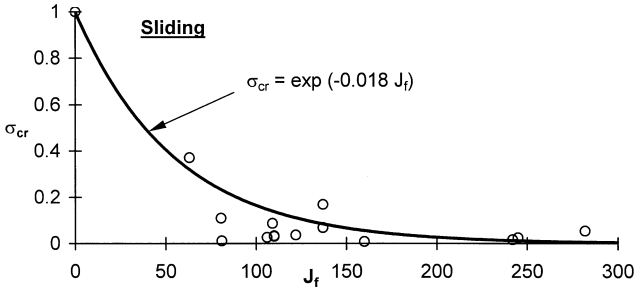

Fig. 12a. Variation of σ_{cr} with J_f for sliding mode of failure

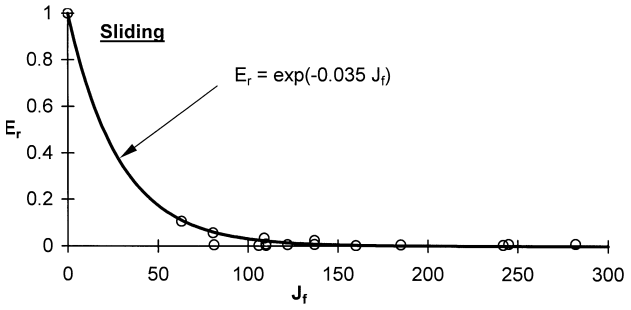

Fig. 12b. Variation of E_r with J_f for sliding mode of failure

ii. For sub-horizontal continuous joints ($\theta \approx 10°$), the failure mode will be sliding if interlocking is nil/low. If interlocking is medium, the failure mode will be shearing. For higher interlocking splitting can be expected to occur.
iii. If the continuous joints dip near 20°, sliding will occur for nil/low interlocking. For medium level of interlocking shearing will occur. For very high interlocking, the mass will fail in splitting.
iv. If the continuous joints dip near 30°, the mass will fail in shearing if interlocking is high or very high. Otherwise, it will fail due to sliding only.
v. In general, if the continuous joints dip by an amount up to 30°, the mode of failure will vary from sliding to splitting depending on combination of interlocking and orientation. For low interlocking, sliding may be assumed and for high interlocking, the mode may be assumed shifting towards shearing and then splitting.
vi. If the dip of the continuous joints is 35° to 65°, sliding is the possible mode of failure irrespective of interlocking conditions of joints.
vii. If the dip of continuous joints is beyond 70°, rotation can be expected to occur. The geometry of the blocks forming the mass will be an important factor. The tendency to rotate will increase with increase of $h/b > 1$.
viii. If the continuous joints are exactly vertical, shearing will be the most probable mode of failure.

Table 4. Coefficients 'a' and 'b' for predicting σ_{cj} and E_j

Failure mode	a	b
Splitting	−0.0123	−0.020
Shearing	−0.0110	−0.020
Rotation	−0.0250	−0.040
Sliding	−0.0180	−0.035

6.2 Prediction of Strength and Modulus of Deformation

Once the probable mode of failure is assigned based on the guidelines suggested above, the value of Joint Factor J_f can be computed for each metre depth of the jointed mass. The maximum value of J_f should be considered as this will represent the weakest zone in the section. The following expressions reproduced from previous sections can be used for computing the average strength and tangent modulus for a mass with two sets of joints:

$$\sigma_{cj} = \sigma_{ci} \exp(\text{a}.J_f), \tag{12}$$

$$E_j = E_i \exp(\text{b}.J_f), \tag{13}$$

where σ_{ci} and E_i are the uniaxial compressive strength and tangent modulus of the intact rock respectively. The values of the coefficients, 'a' and 'b' for different modes of failure are presented in Table 4.

7. Conclusions

Strength and deformation behaviour of a jointed rock mass is a complicated phenomenon due to combinations of modes of failure. To have a correct understanding of the occurrence of various modes of failure and their effect on the engineering response of jointed rock masses an experimental programme was conducted. The findings of this study established four distinct modes of failure namely *splitting* of intact material, *shearing* of intact material, *rotation* of blocks and *sliding* along the critical joints. These modes of failure have been found to be dependent on the configuration of joints and interlocking conditions. Guidelines have been suggested to assess the probable modes of failure in the field based on the mapping of joints. A weakness coefficient called Joint Factor has been used to describe the effect of jointing introduced in the intact rock. Expressions have been suggested to compute the strength and tangent modulus of the jointed mass through the Joint Factor. The methods to compute the Joint Factor for various modes of failure have also been established.

Acknowledgements

The work presented in this paper is a part of the research carried out by the first author under the supervision of the co-authors at IIT Delhi for his PhD degree. The first author is

grateful to the authorities at M.N.R. Engg. College, Allahabad for deputing him to IIT Delhi, and Government of India for providing QIP fellowship for the completion of the PhD.

Special thanks are due to Prof. H. H. Einstein and the two unknown reviewers of this paper for their valuable contribution in reorganising the manuscript.

References

Deere, D. U., Miller, R. P. (1966): Engineering classification and index properties for intact rock. Technical Report No. AFNL-TR-65-116. Air Force Weapons Laboratory, New Mexico.

Ramamurthy, T. (1993): Strength and modulus response of anisotropic rocks. In: Comprehensive rock engineering, vol. 1. Pergamon Press, Oxford, 313–329.

Ramamurthy, T., Arora, V. K. (1994): Strength prediction for jointed rocks in confined and unconfined states. Int. J. Rock Mech. Min. Sci. Geomech. Abstr. 31(1), 9–22.

Singh, M. (1997): Engineering behaviour of jointed model materials. Ph.D. Thesis, IIT, New Delhi, India.

Authors' address: Dr. Mahendra Singh, Civil Engineering Department, Indian Institute of Technology, Roorkee-247 667, INDIA. Email: singhfce@iitr.ernet.in.